NIH Public Access
Author Manuscript
Nat Neurosci. Author manuscript; available in PMC 2006 April 13.

Published in final edited form as:
Nat Neurosci. 2002 March ; 5(3): 210–217.

Differential modulation of $Ca_v2.1$ channels by calmodulin and Ca^{2+}-binding protein 1

Amy Lee[1], **Ruth E. Westenbroek**[1], **Françoise Haeseleer**[2], **Krzysztof Palczewski**[1,3], **Todd Scheuer**[1], and **William A. Catterall**[1]

1*Department of Pharmacology, University of Washington School of Medicine, Seattle, Washington 98195-7280, USA*

2*Department of Opthalmology, University of Washington School of Medicine, Seattle, Washington 98195-7280, USA*

3*Department of Chemistry, University of Washington School of Medicine, Seattle, Washington 98195-7280, USA*

Abstract

$Ca_v2.1$ channels, which mediate P/Q-type Ca^{2+} currents, undergo Ca^{2+}/calmodulin (CaM)-dependent inactivation and facilitation that can significantly alter synaptic efficacy. Here we report that the neuronal Ca^{2+}-binding protein 1 (CaBP1) modulates $Ca_v2.1$ channels in a manner that is markedly different from modulation by CaM. CaBP1 enhances inactivation, causes a depolarizing shift in the voltage dependence of activation, and does not support Ca^{2+}-dependent facilitation of $Ca_v2.1$ channels. These inhibitory effects of CaBP1 do not require Ca^{2+}, but depend on the CaM-binding domain in the α_1 subunit of $Ca_v2.1$ channels ($\alpha_1 2.1$). CaBP1 binds to the CaM-binding domain, co-immunoprecipitates with $\alpha_1 2.1$ from transfected cells and brain extracts, and colocalizes with $\alpha_1 2.1$ in discrete microdomains of neurons in the hippocampus and cerebellum. Our results identify an interaction between Ca^{2+} channels and CaBP1 that may regulate Ca^{2+}-dependent forms of synaptic plasticity by inhibiting Ca^{2+} influx into neurons.

Calcium entry into cells through voltage-gated Ca^{2+} channels initiates a wide range of cellular processes including protein phosphorylation, gene expression and neurotransmitter release[1]. Neuronal Ca^{2+} channels consist of a pore-forming α_1 subunit and auxiliary β, $\alpha_2\delta$ and sometimes γ subunits[2], and their function depends considerably on interactions with additional regulatory factors. For example, the activation of G-protein-coupled receptors by neurotransmitters inhibits $Ca_v2.1$ and $Ca_v2.2$ channels, which mediate P/Q-type and N-type Ca^{2+} currents, respectively, through the binding of G-protein $\beta\gamma$ subunits to distinct sites on the Ca^{2+} channel α_1 subunit[3-5]. These channels are also inhibited by direct interactions with synaptic SNARE (soluble NSF attachment protein receptor proteins)—a process that may optimize coupling between Ca^{2+} entry and synaptic vesicle fusion[6-8]. Characterizing the functional interactions between Ca^{2+} channels and other signaling molecules is therefore crucial to understanding how many Ca^{2+}-dependent processes in neurons are regulated.

We have shown previously that the prominent Ca^{2+} sensor CaM binds to a CaM-binding site (CBD) in the carboxy-terminal domain of the $\alpha_1 2.1$ subunit and mediates the dual feedback regulation of $Ca_v2.1$ channels by Ca^{2+} ions[9,10]. A second site, located amino-terminal to the CBD, is analogous to the IQ domain that mediates Ca^{2+}/CaM-dependent inactivation of Ca_v1 (L-type) channels[11-13]. The IQ domain of $\alpha_1 2.1$ interacts with CaM *in vitro* and also contributes to the regulation of $Ca_v2.1$ channels by CaM[14,15]. Ca^{2+}/CaM mediates both

Correspondence should be addressed to W.A.C. (wcatt@u.washington.edu).

NIH-PA Author Manuscript
NIH-PA Author Manuscript
NIH-PA Author Manuscript

NIH-PA Author Manuscript

NIH-PA Author Manuscript

NIH-PA Author Manuscript

facilitation and enhanced inactivation of $Ca_v2.1$ channels in transfected cells during trains of depolarizations[10,15]. Presynaptic $Ca_v2.1$ channels in the brain undergo similar forms of Ca^{2+}-dependent modulation that can lead to both synaptic facilitation and depression[16-18]. Because $Ca_v2.1$ channels are essential to neurotransmitter release at most central synapses[19,20], regulation by CaM may contribute widely to mechanisms of activity-dependent synaptic plasticity.

Calmodulin is the best characterized member of a superfamily of Ca^{2+}-binding proteins that exhibit four EF-hand motifs, one or more of which may be nonfunctional in the coordination of Ca^{2+} (ref. 21). Included in this superfamily are the neuronal Ca^{2+}-binding proteins (NCBPs) that, unlike CaM, are localized primarily in neurons[22]. Some NCBPs can substitute for CaM *in vitro*[23,24], which suggests that NCBPs may regulate effectors that are typically thought to be modulated by CaM. Here we have studied the interaction of CaBP1, an NCBP located in the retina and brain[25], with $Ca_v2.1$ channels. We show that CaBP1 binds to the CBD of the $\alpha_1 2.1$ subunit, but with properties and functional consequences that are different from those of CaM. Our findings expand the repertoire of modulatory interactions that take place between Ca^{2+} channels and Ca^{2+}-binding proteins and indicate that NCBPs, in addition to CaM, may have a role in the activity-dependent regulation of neuronal Ca^{2+} influx.

RESULTS

CaBP1 interacts with the CBD of $\alpha_1 2.1$

Although CaBP1 is a neuron-specific Ca^{2+}-binding protein that shares nearly 56% amino acid sequence identity with CaM[25], it differs in having a consensus site for N-terminal myristoylation, an alternatively spliced region, inactivating amino acid substitutions in the second of the four EF-hand motifs, and an extra turn in the helical domain that links the N- and C-terminal lobes (Fig. 1a). To determine whether CaBP1 can substitute for CaM in interactions with $Ca_v2.1$ channels, we tested the ability of CaBP1 to interact with various intracellular domains of the $\alpha_1 2.1$ subunit. In yeast two-hybrid assays, CaBP1 activated transcription of *HIS3* and *lacZ* reporter genes only in yeast that had been cotransformed with $\alpha_1 2.1$ constructs that included the CBD (Fig. 1b and **c**). CaBP1 did not interact with the IQ domain or with a control plasmid that lacked the CaBP1 coding region. These results indicated that CaBP1 may modulate $Ca_v2.1$ channel function through interactions with the CBD.

To confirm that CaBP1 associated with the CBD in the intact channel, we tested whether CaBP1 co-immunoprecipitated with $Ca_v2.1$ channels from cotransfected tsA-201 cells. In this assay, CaM co-immunoprecipitates with $\alpha_1 2.1$ in a Ca^{2+}-dependent manner only when the cells are exposed to Ca^{2+} ionophore[9]. Under these conditions CaBP1 also co-immunoprecipitated with $\alpha_1 2.1$. When Ca^{2+} was buffered with 10 mM EGTA, however, the association of CaBP1 with the channel was not affected (Fig. 2a). This co-immunoprecipitation of CaBP1 was specific because CaBP1 was not immunoprecipitated with control IgG or with $\alpha_1 2.1$-specific antibodies in cells transfected with CaBP1 alone, and CaBP1 did not co-immunoprecipitate with $\alpha_1 2.1$ subunits that lacked the CBD. Thus, despite its Ca^{2+} independence, the interaction between CaBP1 and $Ca_v2.1$ channels requires the same intracellular domain of $Ca_v2.1$ that binds CaM.

CaBP1 associates with neuronal $Ca_v2.1$ channels

To determine whether CaBP1 associated with endogenous $Ca_v2.1$ Ca^{2+} channels, co-immunoprecipitation experiments were done with extracts from rat cerebellum, which contains high concentrations of $\alpha_1 2.1$ and CaBP1 mRNA[25,26]. Immunoblots of CaBP1 showed two proteins (28 and 36 kDa) that specifically co-immunoprecipitated with $\alpha_1 2.1$ (Fig. 2b, left) but not with control IgG (Fig. 2b, middle). The 36-kDa species might represent caldendrin, a larger isoform of CaBP1 that is produced from alternative splicing[25,27]. The 28-kDa species was

NIH-PA Author Manuscript

NIH-PA Author Manuscript

NIH-PA Author Manuscript

consistent in size with the predicted molecular mass of the long CaBP1 isoform that we used in transfected cells (Fig. 2b, right), in support of a physiological interaction between neuronal $Ca_v2.1$ channels and CaBP1.

To identify the potential cellular sites of interaction between CaBP1 and $\alpha_1 2.1$, we immunostained rat brain sections with antibodies specific for both proteins. Compared with the immunostaining of $\alpha_1 2.1$, the immunostaining for CaBP1 was generally far more restricted within the brain and more commonly associated with somatodendritic regions than with nerve terminals. However, CaBP1 and $\alpha_1 2.1$ showed similar patterns of punctate staining in the CA1 region of the hippocampus and in the molecular layer of the cerebellum (Fig. 3a–f). As a large proportion of punctate labeling of $\alpha_1 2.1$ in the cerebellum colocalizes with that of syntaxin[28], it is likely that CaBP1 and $Ca_v2.1$ channels coexist in at least some presynaptic nerve terminals. Immunostaining for CaBP1 and for $\alpha_1 2.1$ also overlapped in clusters along the dendrites of cerebellar Purkinje neurons and in structures that resembled dendritic spines (data not shown), however, which suggests that CaBP1 may associate with $Ca_v2.1$ channels in the post- as well as in the presynaptic membrane.

CaBP1 enhances inactivation of $Ca_v2.1$ channels

To elucidate the functional consequences of the interaction between CaBP1 and $Ca_v2.1$ channels, we determined the effect of CaBP1 on Ca^{2+} currents (I_{Ca}) in whole-cell patch-clamp recordings of transfected tsA-201 cells. We first compared the effects of transfected CaBP1 and endogenous CaM on inactivation of I_{Ca}. We have shown previously that Ca^{2+Ca}/CaM enhances the inactivation of I_{Ca} during step depolarizations when intracellular recording solutions contain 0.5 mM EGTA[9,10]. Here, inactivation of I_{Ca} caused by Ca^{2+}/CaM proceeded with a single exponential time course ($\tau = 852.3 \pm 63.7$ ms at +20 mV, $n = 18$) that was relatively insensitive to the test voltage (Fig. 4a and **b**). By contrast, CaBP1 caused I_{Ca} to decay significantly faster than in cells that were transfected with only $Ca_v2.1$.

In almost all of the cells that were cotransfected with CaBP1, the decay of I_{Ca} evoked by +20- and +30-mV pulses was best fit by a double exponential function, with a slow component similar to control and a fast component comprising 30–40% of the peak current (Fig. 4c). With a +10-mV test pulse, however, biphasic inactivation was detected in only 11 out of 20 cells that had been cotransfected with CaBP1. At this test voltage, which elicits the peak inward I_{Ca}, Ca^{2+}/CaM-dependent inactivation is maximal[10]. Therefore, the absence of a fast phase of inactivation in some cells cotransfected with CaBP1 might have resulted from more effective competition by Ca^{2+}/CaM.

Competition between CaM and CaBP1 for $Ca_v2.1$ channels was supported further by the observation of a marked reduction in Ca^{2+}-dependent inactivation in cells cotransfected with CaBP1 (Fig. 5a and **b**). Enhanced inactivation caused by CaM results in a significant reduction in the residual current at the end of a 1-second depolarizing test pulse normalized to the peak current (I_{res}/I_{pk}) for I_{Ca} as compared with I_{Ba} (refs. 9, 10). By contrast, in cells cotransfected with CaBP1, I_{res}/I_{pk} was already reduced when Ba^{2+} was the charge carrier and was not significantly different for I_{Ca} and I_{Ba} (Fig. 5a and **b**). Ca^{2+}-dependent inactivation was not affected in the same way by cotransfection with CaM instead of CaBP1, which indicated that the faster, Ca^{2+}-independent inactivation was a specific consequence of the modulation of $Ca_v2.1$ channels by CaBP1.

To clarify the effects of CaBP1 on fast inactivation of $Ca_v2.1$ channels, we measured the amplitude of I_{Ca} at the 200-ms time point during a 1-s test pulse and normalized this to the peak current (I_{200}/I_{pk}, Fig. 5c and **d**). We used more positive test voltages to limit Ca^{2+} entry, thus minimizing the contribution of endogenous CaM in these experiments. With 0.5 mM EGTA, faster inactivation of I_{Ca} in cells with CaBP1 caused a significant decrease in I_{200}/I_{pk}

NIH-PA Author Manuscript

NIH-PA Author Manuscript

NIH-PA Author Manuscript

(0.45 ± 0.06 for CaBP1 versus 0.79 ± 0.03 for control, $p < 0.01$). CaBP1 significantly enhanced fast inactivation of I_{Ba} (I_{200}/I_{pk} of 0.43 ± 0.09 for CaBP1 versus 0.74 ± 0.07 for control, $p < 0.05$) and also of I_{Ca} with 10 mM of the intracellular calcium chelator BAPTA (I_{200}/I_{pk} of 0.56 ± 0.08 for CaBP1 versus 0.85 ± 0.03 for control, $p < 0.02$). The CBD was essential for these effects on inactivation, because CaBP1 had no effect on channels in which this domain had been deleted (Fig. 5c and **d**, $Ca_v2.1_{\Delta CBD}$; $p > 0.3$). Together with biochemical analyses, these results support a Ca^{2+}-independent association of CaBP1 with the CBD, which mediates a strong acceleration of $Ca_v2.1$ channel inactivation that does not require Ca^{2+} influx or intracellular accumulation of Ca^{2+}.

CaBP1 shifts voltage dependence of $Ca_v2.1$ activation

In cells cotransfected with CaBP1 and $Ca_v2.1$, the normalized tail current–voltage curve was shifted positively and was shallower than in cells transfected with $Ca_v2.1$ alone (Fig. 6a). CaBP1 caused significant increases in the half-activation voltage, $V_{1/2}$ (12.8 ± 1.3 mV for CaBP1 versus 4.5 ± 0.9 mV for control, $p < 0.01$), and slope factor of the tail current–voltage curve (−8. 7 ± 0.5 mV for CaBP1 versus −5.2 ± 0.6 mV for control, $p < 0.01$). Similar to the other actions of CaBP1 on $Ca_v2.1$ channels, these effects on I_{Ca} activation were essentially reproduced with intracellular BAPTA and extracellular Ba^{2+} but were not observed with $Ca_v2.1_{\Delta CBD}$ channels (Fig. 6b–d), which indicates that the Ca^{2+}-independent association of CaBP1 with the CBD results in a newly identified, multifaceted regulation of $Ca_v2.1$ channels.

Ca^{2+}-dependent facilitation is not supported by CaBP1

Activity-dependent increases in intracellular Ca^{2+} cause an initial facilitation of I_{Ca} owing to the interaction of Ca^{2+}/CaM with $Ca_v2.1$ channels (refs 10, 15). This Ca^{2+}-dependent facilitation was evident with 0.5 mM intracellular EGTA in paired-pulse protocols, in which Ca^{2+} influx during a short prepulse induced a significant increase in the tail current elicited by a subsequent test pulse (Fig. 7a). With the same voltage protocol, no facilitation of I_{Ca} was observed in cells cotransfected with CaBP1 (Fig. 7b). Because of the strong voltage-dependent enhancement of I_{Ca} inactivation caused by CaBP1, it was possible that paired-pulse facilitation in cells cotransfected with CaBP1 might have been obscured by the onset of inactivation during the conditioning prepulse. Alternatively, CaBP1, unlike CaM, might not support Ca^{2+}-dependent facilitation of I_{Ca}.

To distinguish between these possibilities, we analyzed the properties of I_{Ca} during trains of short (5-ms) repetitive depolarizations, which should initially minimize the impact of voltage-dependent inactivation and reveal facilitation of I_{Ca} early in the train. With 0.5 mM intracellular EGTA, $Ca_v2.1$ Ca^{2+} currents undergo a sustained facilitation and gradually inactivate below initial current amplitudes after 800 ms of repetitive pulses (Fig. 7c), an effect that depends on Ca^{2+}/CaM[10]. In cells cotransfected with CaBP1, facilitation of I_{Ca} was reduced markedly, with current amplitudes rapidly inactivating below initial values only 200 ms into the train (Fig. 7c).

The maximum facilitated I_{Ca} amplitude at 50 ms in cells cotransfected with CaBP1 (1.04 ± 0.02, $n = 13$) was not significantly different from the Ca^{2+}-independent facilitation of Ba^{2+} currents in cells transfected with $Ca_v2.1$ alone (1.04 ± 0.03, $n = 5$, $p = 0.80$) or cotransfected with CaBP1 (1.02 ± 0.02, $n = 11$, $p = 0.52$; Fig. 7d), which indicated that CaBP1 does not support Ca^{2+}-dependent facilitation of $Ca_v2.1$ channels. Together with the enhanced inactivation and positive shifts in activation caused by CaBP1, the absence of Ca^{2+}-dependent facilitation would strongly limit voltage-dependent Ca^{2+} entry through $Ca_v2.1$ channels. These results highlight further the different modulation of these Ca^{2+} channels by CaBP1 and CaM.

NIH-PA Author Manuscript

NIH-PA Author Manuscript

NIH-PA Author Manuscript

Discussion

We have shown that the neuronal Ca^{2+}-binding protein CaBP1 interacts with and modulates $Ca_v2.1$ channels in a manner that is markedly different from that of CaM. CaBP1 bound to the CBD of $\alpha_1 2.1$ but caused significantly faster inactivation of $Ca_v2.1$ channel currents than that caused by CaM. CaBP1 also positively shifted tail current-activation curves and did not support Ca^{2+}-dependent facilitation of $Ca_v2.1$ currents. Neither the association of CaBP1 with the CBD nor the inhibitory modulation by CaBP1 required Ca^{2+}, in contrast to the effects of CaM on $Ca_v2.1$ channels, which are strictly dependent on Ca^{2+}. The observed association and colocalization of CaBP1 and $Ca_v2.1$ channels in neurons in the brain suggest that Ca^{2+} channel regulation by CaBP1 may be an important determinant of Ca^{2+} signaling pathways in neurons.

Ca^{2+}-independent binding and modulation by CaBP1

The Ca^{2+} independence of the interaction between CaBP1 and $Ca_v2.1$ was unexpected given the previously observed Ca^{2+}-dependent association of CaBP1 with other CaM targets[25]. It is possible that very local rises in Ca^{2+} might have escaped buffering by BAPTA in our experiments, which could have been sufficient for binding to CaBP1 and for causing Ca^{2+}-dependent modulation of I_{Ca}. This possibility seems unlikely, however, because the modulation by CaBP1 did not change appreciably when Ba^{2+} was the permeant ion; Ba^{2+} ions bind to EF-hand motifs with relatively low affinity and so should not reproduce Ca^{2+}-dependent regulation of target molecules[29].

Calcium-free CaM can associate with and regulate several targets, including the ryanodine receptor RyR1, cyclic GMP kinase and a CaM-dependent adenylyl cyclase from *Bordetella pertussis*[30-32]. In addition, GCAPs—photoreceptor Ca^{2+}-binding proteins—activate guanylyl cyclases in their Ca^{2+}-free forms[33,34]. Thus, CaBP1 might have a similar flexibility and interact with and regulate some effectors without binding Ca^{2+}. Although we cannot exclude the possibility that CaBP1 may modulate some aspects of Ca^{2+} channel function in a Ca^{2+}-dependent manner, we found no evidence to support a requirement for Ca^{2+} in the effects of CaBP1 on the activation and inactivation of $Ca_v2.1$ channels. Thus, despite the Ca^{2+}-sensing capability of CaBP1, we propose that CaBP1 itself does not mediate Ca^{2+}-dependent regulation of $Ca_v2.1$ channels, but might indirectly influence feedback regulation by Ca^{2+} by competing with CaM. Thus, CaBP1 may act more like auxiliary Ca^{2+} channel β-subunits by altering the intrinsic properties of $Ca_v2.1$ channels to fine-tune voltage-gated Ca^{2+} entry in specific classes of neurons.

Distinct modulation of $Ca_v2.1$ by CaBP1 and CaM

We have shown that both CaM and CaBP1 interact with the CBD of the $\alpha_1 2.1$ subunit and that this site is essential for full channel regulation by both proteins. Conflicting evidence indicates that the IQ domain—a sequence that is N-terminal to the CBD—is involved in the modulation of $Ca_v2.1$ channels by Ca^{2+}/CaM[15]. Our results do not support the importance of the IQ domain in modulation by CaBP1 because, first, CaBP1 interacted with the CBD but not the IQ domain in yeast two-hybrid assays (Fig. 1b and **c**); second, deleting the CBD prevented the co-immunoprecipitation of CaBP1 with $\alpha_1 2.1$ (Fig. 2a); and third, the fast inactivation and shifts in the voltage dependence of activation caused by CaBP1 were abolished in channels that lacked the CBD (**Figs.** 5 and 6). Notably, removing the CBD from $\alpha_1 2.1$ eliminated regulation by CaBP1 more completely than it eliminated regulation by CaM[10]. Together, our results indicate that the CBD may be the primary determinant for the functional effects of CaBP1 on $Ca_v2.1$ channels.

If both CaM and CaBP1 interact with the CBD, how is it that CaBP1 causes Ca^{2+}-independent fast inactivation and positively shifted activation, whereas CaM causes Ca^{2+}-dependent

NIH-PA Author Manuscript

NIH-PA Author Manuscript

NIH-PA Author Manuscript

facilitation and inactivation of $Ca_v2.1$ channels? One possibility is that key structural features that distinguish CaBP1 from CaM, such as its extra-long central helical domain and N-terminal myristoylation (Fig. 1a), may permit Ca^{2+}-independent binding of CaBP1 to the CBD, which might then lead to its unique inhibitory modulation of I_{Ca}. Future experiments that determine how such differences between CaBP1 and CaM contribute to specific forms of $Ca_v2.1$ regulation may reveal how ion channels and other signaling molecules are differentially modulated by CaM and related Ca^{2+}-binding proteins.

Modulation of neuronal $Ca_v2.1$ channels by CaBP1

Our immunoprecipitation and immunofluorescence studies showed that CaBP1 and $\alpha_1 2.1$ associate physically in extracts of rat cerebellum and that their subcellular distributions overlap in this brain region, which indicates that CaBP1 may have a physiological role in the regulation of $Ca_v2.1$ channels. Because both CaM and CaBP1 interacted with the same site on the $\alpha_1 2.1$ subunit, an important issue is whether $Ca_v2.1$ would interact functionally with CaM and/or CaBP1 in neurons in which both Ca^{2+}-binding proteins are expressed.

Although we do not know whether CaM and CaBP1 bind simultaneously to $Ca_v2.1$ channels, our electrophysiological studies suggested that CaM and CaBP1 might competitively regulate the channel. CaBP1 more strongly enhanced inactivation of I_{Ca} when the influence of Ca^{2+}/CaM was suppressed either with extracellular Ba^{2+} or intracellular BAPTA, or with test voltages that elicited submaximal Ca^{2+} influx. These results imply that when intracellular Ca^{2+} concentrations are high $Ca_v2.1$ channels may be facilitated predominantly by CaM, and that the inactivating effects of CaBP1 become most prominent when cytoplasmic Ca^{2+} concentrations decline. In this way, CaM and CaBP1 may coordinately act as a molecular switch to intensify neuronal Ca^{2+} influx in response to activity-dependent alterations in intracellular concentrations of Ca^{2+}.

NCBPs and synaptic transmission

Emerging evidence supports a role for NCBPs in the regulation of synaptic transmission. In particular, neuronal Ca^{2+} sensor-1 (NCS-1), which is more distantly related to CaM than is CaBP1, regulates neurotransmitter release[35], synapse formation[36] and neuronal circuits that control associative learning[37]. Notably, NCS-1 has been implicated in the negative regulation of Ca^{2+} channels in chromaffin cells[38], which suggests that $Ca_v2.1$ channels may be modulated by NCBPs in addition to CaBP1.

Given the widespread distribution of $Ca_v2.1$ channels throughout the nervous system, the cell type–specific modulation of $Ca_v2.1$ by CaBP1, CaM or other NCBPs may fundamentally determine the nature of presynaptic and postsynaptic Ca^{2+} signals and the functional consequences of synaptic activity.

Methods

Yeast two-hybrid assays. We amplified cDNAs encoding the long isoform of human CaBP1 (ref. 25) and the cytoplasmic domains of $\alpha_1 2.1$ by polymerase chain reaction and subcloned them into the yeast two-hybrid vectors pACT2 and pAS2-1, respectively (Clontech, Palo Alto, California). To test for interactions between CaBP1 and specific domains of $\alpha_1 2.1$, the corresponding plasmids were cotransformed into yeast strain Y190. We assayed growth on medium lacking histidine and β-galactosidase to identify interacting proteins as described[9].

Cell culture and transfection. We grew tsA-201 cells to ~70% confluency and transfected them by the calcium phosphate method with an equimolar ratio of cDNAs encoding the rat brain Ca^{2+} channel subunits $\alpha_1 2.1$ (rbA), β_{2a} and $\alpha_2\delta$ (ref. 26). The $\alpha_1 2.1$ construct that lacks

NIH-PA Author Manuscript

NIH-PA Author Manuscript

NIH-PA Author Manuscript

amino acids 1969–2000 ($\alpha_1 2.1_{\Delta CBD}$) has been described[10]. The long isoform of human CaBP1 (ref. 25) was subcloned into the *Bam*HI sites of pcDNA3.1+ (Invitrogen, Carlsbad, California) and transfected at a 5:1 molar excess with Ca^{2+} channel subunits. For electrophysiological experiments, we plated cells on 35-mm dishes and transfected them with 5 μg of total DNA, including 0.3 μg of a CD8 expression plasmid to allow the detection of transfected cells. For co-immunoprecipitation assays, we plated cells on 150-mm dishes and transfected them with 50 μg of total plasmid DNA.

Co-immunoprecipitation assays. At least 48 h after transfection, tsA-201 cells were homogenized in ice-cold lysis buffer (1% Nonidet P-40 in TBS (20 mM Tris-HCl, pH 7.3, 150 mM NaCl), 10 mM EGTA and protease inhibitors) and centrifuged at 1,000*g* for 5 min. To maintain Ca^{2+}-dependent interactions, we pretreated some groups with 5 μM A23187 and 2 mM $CaCl_2$ for 15 min but did not include EGTA in the lysis buffer. The postnuclear supernatant (300–400 μg of membrane protein) was incubated with 15 μg of $\alpha_1 2.1$-specific antibodies (raised against CNA5)[39] for 2 h at 4°C. Immune complexes were separated on protein A–Sepharose, resolved by SDS–PAGE and transferred to nitrocellulose. For immunoblotting, we blocked nitrocellulose filters for 30 min in 5% milk/TBS and incubated them with the CaBP1 antiserum UW72 (ref. 25; 1:1,000 dilution) or with CNA5-specific antibodies (2.5 μg/ml) for 1 h. Blots were washed three times in TBS with 0.05% Tween 20 (TBST) and incubated with horse-radish peroxidase–linked protein A (Amersham, Piscataway, New Jersey; 1:2,000) for 40 min. We used ECL western blotting reagent (Amersham) for detection of chemiluminescence.

For co-immunoprecipitations from rat brain, we homogenized cerebellar tissue from two adult male rats in 0.3 M sucrose, 75 mM NaCl, 10 mM Tris-HCl, pH 7.4, and 10 mM EGTA. We included protease inhibitors in the homogenization buffer and in buffers used at all subsequent steps. Homogenates were centrifuged for 10 min at 1,000*g*, and membrane fractions were separated from the postnuclear supernatant at 100,000*g* for 30 min. Membrane proteins were solubilized with 4 ml of buffer A (1% Triton X-100, 10 mM Tris, pH 7.4, and 10 mM EGTA) and insoluble material was removed by further centrifugation (100,000*g* for 30 min). Ca^{2+} channels were immunoprecipitated with 15 μg of CNA5-specific antibodies per ml of solubilized membrane protein. We isolated immune complexes on protein A–Sepharose and detected the associated CaBP1 by immunoblotting as described above.

Immunocytochemistry. Anesthetized adult Sprague–Dawley rats were perfused intracardially with 4% paraformaldehyde in 0.1 M sodium phosphate buffer, pH 7.4. The brain was post-fixed and cryoprotected in 30% (w/v) sucrose, and tissue sections (35 μm) were cut on a sliding microtome in 0.1 M phosphate buffer. Tissue sections were rinsed with 0.1 M Tris-buffered saline (TBS) and blocked sequentially with 2% avidin and 2% biotin. For the double-labeling of CaBP1 and $\alpha_1 2.1$, we incubated tissue sections in UW72 antiserum (diluted 1:100) for 36 h at 4°C, biotinylated goat antibody against rabbit IgG (Vector Laboratories, Burlingame, California; 1:300) for 1 h at 37°C, and avidin D–fluorescein (Vector Laboratories; 1:300) for 1 h at 37°C, with rinsing between each step. The tissue was then blocked with 5% normal rabbit serum in TBS for 1 h and incubated with affinity-purified Fab fragments for 1 h at 37°C. After rinsing, tissue sections were incubated with antibodies specific for CNA5 (1:15) for 36 h at 4°C, biotinylated goat antibody against rabbit IgG (1:300) for 1 h at 37°C, and avidin D–Texas Red (1:300) for 1 h at 37°C. Tissue sections were mounted on gelatin-coated slides, protected with coverslips, and viewed with a Bio-Rad MRC 600 microscope in the W.M. Keck Imaging Facility at the University of Washington. All procedures conformed to protocols approved by the Animal Welfare Committee of the University of Washington.

Electrophysiology and data analysis. At least 48 h after transfection, tsA-201 cells were incubated with CD8-specific antibody–coated microspheres (Dynal, Oslo, Norway) to permit

NIH-PA Author Manuscript

NIH-PA Author Manuscript

NIH-PA Author Manuscript

detection of transfected cells. We recorded whole-cell Ca^{2+} currents with a List EPC-7 patch-clamp amplifier and filtered them at 5 kHz. Leak and capacitive transients were subtracted using a P/–4 protocol. Extracellular recording solutions were composed of 150 mM Tris, 1 mM $MgCl_2$ and 10 mM $CaCl_2$ or $BaCl_2$; intracellular solutions were composed of 120 mM *N*-methyl-D-glucamine, 60 mM HEPES, 1 mM $MgCl_2$, 2 mM Mg-ATP and 0.5 mM EGTA or 10 mM BAPTA. The pH of all solutions was adjusted to 7.3 with methanesulfonic acid.

The time course of I_{Ca} decay was fit by either $A[\exp(-t/\tau)]$ or $A_{slow}[\exp(-t/\tau_{slow})] + A_{fast}[\exp(t/\tau_{fast})]$, where t is time; A_{slow} and A_{fast} are the amplitudes of the slow and fast exponentials, respectively, at $t = 0$; and τ_{slow} and τ_{fast} are the time constants of the decay of the two processes. Normalized tail current–voltage curves were fit with a single Boltzmann function: $A/\{1 + \exp[(V - V_{1/2})/k] + b\}$, where V is test pulse voltage, $V_{1/2}$ is the midpoint of the activation curve, k is a slope factor, A is the amplitude and b is the baseline. Curve fits and data analysis were done with Igor Pro software (Wavemetrics, Lake Oswego, Oregon). All averaged data are the mean ± s.e.m. We determined the statistical significance of differences between groups by Student's *t*-test (SigmaPlot, SPSS Science, Chicago, Illinois).

Acknowledgements

This work was supported by NIH Research Grant R01 NS22625 to W.A.C, a NSRA postdoctoral research fellowship from NIH (F32 NS10645) to A.L., NIH Research Grant R01 EY08061 to K.P. and research grants from Research to Prevent Blindness, Inc., the Alcon Research Institute and the E.K. Bishop Foundation to K.P.

References

1. Miller RJ. Multiple calcium channels and neuronal function. Science 1987;235:46–52. [PubMed: 2432656]
2. Catterall WA. Structure and function of neuronal Ca^{2+} channels and their role in neurotransmitter release. Cell Calcium 1998;24:307–323. [PubMed: 10091001]
3. Ikeda SR. Voltage-dependent modulation of N-type calcium channels by G-protein βγ subunits. Nature 1996;380:255–258. [PubMed: 8637575]
4. Herlitze S, et al. Modulation of Ca^{2+} channels by G protein βγ subunits. Nature 1996;380:258–262. [PubMed: 8637576]
5. De Waard M, et al. Direct binding of G-protein βγ complex to voltage-dependent calcium channels. Nature 1997;385:446–450. [PubMed: 9009193]
6. Bezprozvanny I, Scheller RH, Tsien RW. Functional impact of syntaxin on gating of N-type and Q-type calcium channels. Nature 1995;378:623–626. [PubMed: 8524397]
7. Zhong H, Yokoyama CT, Scheuer T, Catterall WA. Reciprocal regulation of P/Q-type Ca^{2+} channels by SNAP-25, syntaxin and synaptotagmin. Nat. Neurosci 1999;2:939–941. [PubMed: 10526329]
8. Wiser O, Bennett MK, Atlas D. Functional interaction of syntaxin and SNAP-25 with voltage-sensitive L- and N-type Ca^{2+} channels. EMBO J 1996;15:4100–4110. [PubMed: 8861939]
9. Lee A, et al. Ca^{2+}/calmodulin binds to and modulates P/Q-type calcium channels. Nature 1999;339:155–159. [PubMed: 10335845]
10. Lee A, Scheuer T, Catterall WA. Ca^{2+}/calmodulin-dependent facilitation and inactivation of P/Q-type Ca^{2+} channels. J. Neurosci 2000;20:6830–6838. [PubMed: 10995827]
11. Qin N, Olcese R, Bransby M, Lin T, Birnbaumer L. Ca^{2+}-induced inhibition of the cardiac Ca^{2+} channel depends on calmodulin. Proc. Natl. Acad. Sci. USA 1999;96:2435–2438. [PubMed: 10051660]
12. Peterson BZ, DeMaria CD, Yue DT. Calmodulin is the Ca^{2+} sensor for Ca^{2+}-dependent inactivation of L-type calcium channels. Neuron 1999;22:549–558. [PubMed: 10197534]
13. Zühlke RG, Pitt GS, Deisseroth K, Tsien RW, Reuter H. Calmodulin supports both inactivation and facilitation of L-type calcium channels. Nature 1999;399:159–161. [PubMed: 10335846]
14. Pate P, et al. Determinants for calmodulin binding on voltage-dependent Ca^{2+} channels. J. Biol. Chem 2000;275:39786–39792. [PubMed: 11005820]

NIH-PA Author Manuscript

NIH-PA Author Manuscript

NIH-PA Author Manuscript

15. DeMaria CD, Soong T, Alseikhan BA, Alvania RS, Yue DT. Calmodulin bifurcates the local Ca^{2+} signal that modulates P/Q-type Ca^{2+} channels. Nature 2001;411:484–489. [PubMed: 11373682]
16. Forsythe ID, Tsujimoto T, Barnes-Davies M, Cuttle MF, Takahashi T. Inactivation of presynaptic calcium current contributes to synaptic depression at a fast central synapse. Neuron 1998;20:797–807. [PubMed: 9581770]
17. Cuttle MF, Tsujimoto T, Forsythe ID, Takahashi T. Facilitation of the presynaptic calcium current at an auditory synapse in rat brainstem. J. Physiol. (Lond.) 1998;512:723–729. [PubMed: 9769416]
18. Borst JG, Sakmann B. Facilitation of presynaptic calcium currents in the rat brainstem. J. Physiol. (Lond.) 1998;513:149–155. [PubMed: 9782166]
19. Dunlap K, Luebke JI, Turner TJ. Exocytotic Ca^{2+} channels in mammalian central neurons. Trends Neurosci 1995;18:89–98. [PubMed: 7537420]
20. Wheeler DB, Randall A, Tsien RW. Roles of N-type and Q-type Ca^{2+} channels in supporting hippocampal synaptic transmission. Science 1994;264:107–111. [PubMed: 7832825]
21. Polans A, Baehr W, Palczewski K. Turned on by Ca^{2+}! The physiology and pathology of Ca^{2+}-binding proteins in the retina. Trends Neurosci 1996;19:547–554. [PubMed: 8961484]
22. Burgoyne RD, Weiss JL. The neuronal calcium sensor family of Ca^{2+}-binding proteins. Biochem. J 2001;353:1–12. [PubMed: 11115393]
23. Sallese M, et al. The G-protein-coupled receptor kinase GRK4 mediates homologous desensitization of metabotropic glutamate receptor 1. FASEB J 2000;14:2569–2580. [PubMed: 11099476]
24. Schaad NC, et al. Direct modulation of calmodulin targets by the neuronal calcium sensor NCS-1. Proc. Natl. Acad. Sci. USA 1996;93:9253–9258. [PubMed: 8799187]
25. Haeseleer F, et al. Five members of a novel Ca^{2+}-binding protein (CABP) subfamily with similarity to calmodulin. J. Biol. Chem 2000;275:1247–1260. [PubMed: 10625670]
26. Stea A, et al. The localization and functional properties of a rat brain α_{1A} calcium channel reflect similarities to neuronal Q- and P-type channels. Proc. Natl. Acad. Sci. USA 1994;91:10576–10580. [PubMed: 7524096]
27. Seidenbecher CI, et al. Caldendrin, a novel neuronal calcium-binding protein confined to the somato-dendritic compartment. J. Biol. Chem 1998;273:21324–21331. [PubMed: 9694893]
28. Westenbroek RE, et al. Immunochemical identification and subcellular distribution of the α_{1A} subunits of brain calcium channels. J. Neurosci 1995;15:6403–6418. [PubMed: 7472404]
29. Chao SH, Suzuki Y, Zysk JR, Cheung WY. Activation of calmodulin by various metal cations as a function of ionic radius. Mol. Pharmacol 1984;26:75–82. [PubMed: 6087119]
30. Rodney GG, Williams BY, Strasburg GM, Beckingham K, Hamilton SL. Regulation of RYR1 activity by Ca^{2+} and calmodulin. Biochemistry 2000;39:7807–7812. [PubMed: 10869186]
31. Yamaki T, Hidaka H. Ca^{2+}-independent stimulation of cyclic GMP-dependent protein kinase by calmodulin. Biochem. Biophys. Res. Commun 1980;94:727–733. [PubMed: 6249290]
32. Greenlee DV, Andreasen TJ, Storm DR. Calcium-independent stimulation of *Bordetella pertussis* adenylate cyclase. Biochemistry 1982;21:2759–2764. [PubMed: 6284209]
33. Rudnicka-Nawrot M, et al. Changes in biological activity and folding of guanylate cyclase-activating protein 1 as a function of calcium. Biochemistry 1998;37:248–257. [PubMed: 9425045]
34. Haeseleer F, et al. Molecular characterization of a third member of the guanylyl cyclase-activating protein subfamily. J. Biol. Chem 1999;274:6526–6535. [PubMed: 10037746]
35. McFerran BW, Graham ME, Burgoyne RD. Neuronal Ca^{2+} sensor 1, the mammalian homologue of frequenin, is expressed in chromaffin and PC12 cells and regulates neurosecretion from dense-core granules. J. Biol. Chem 1998;273:22768–22772. [PubMed: 9712909]
36. Chen XL, et al. Overexpression of rat neuronal calcium sensor-1 in rodent NG108-15 cells enhances synapse formation and transmission. J. Physiol. (Lond.) 2001;532:649–659. [PubMed: 11313436]
37. Gomez M, et al. Ca^{2+} signaling via the neuronal calcium sensor-1 regulates associative learning and memory in *C. elegans*. Neuron 2001;30:241–248. [PubMed: 11343658]
38. Weiss JL, Archer DA, Burgoyne RD. Neuronal Ca^{2+} sensor-1/frequenin functions in an autocrine pathway regulating Ca^{2+} channels in bovine adrenal chromaffin cells. J. Biol. Chem 2000;275:40082–40087. [PubMed: 11006299]

NIH-PA Author Manuscript

NIH-PA Author Manuscript

NIH-PA Author Manuscript

39. Sakurai T, Westenbroek RE, Rettig J, Hell J, Catterall WA. Biochemical properties and subcellular distribution of the BI and rbA isoforms of α_{1A} subunits of brain calcium channels. J. Cell Biol 1996;134:511–528. [PubMed: 8707834]

NIH-PA Author Manuscript

NIH-PA Author Manuscript

NIH-PA Author Manuscript

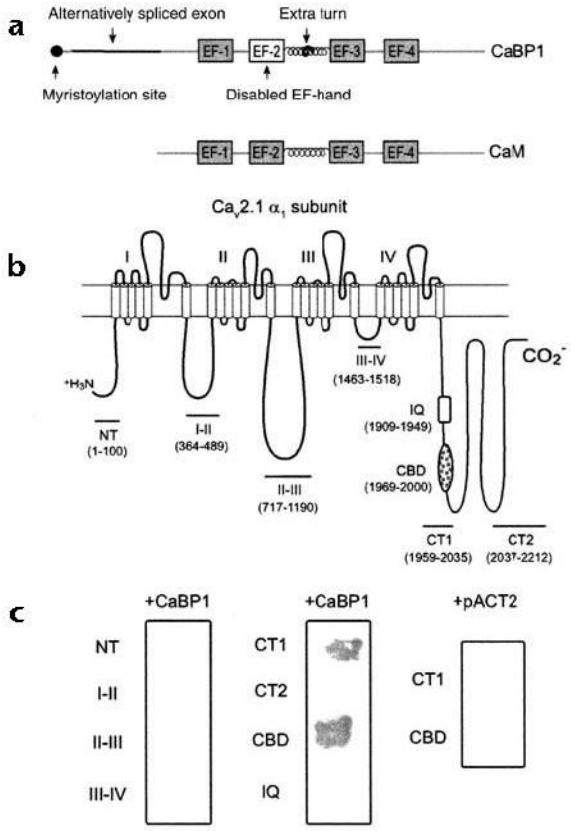

Fig. 1.

CaBP1 binds specifically to the CBD of $\alpha_1$2.1. (**a**) Diagram of CaBP1 and CaM. The four Ca^{2+}-binding EF-hand motifs are shown as boxes, and key structural differences between CaBP1 and CaM are indicated by arrows. (**b**) Diagram of the rat brain $\alpha_1$2.1 subunit (rbA) showing the intracellular domains that were tested for interaction with CaBP1 in yeast two-hybrid assays. The amino acid boundaries of the indicated constructs are given in parentheses. (**c**) β-galactosidase assays of yeast cotransformed with the $\alpha_1$2.1 constructs shown in (**b**) and either CaBP1 or control vector (pACT2).

NIH-PA Author Manuscript
NIH-PA Author Manuscript
NIH-PA Author Manuscript

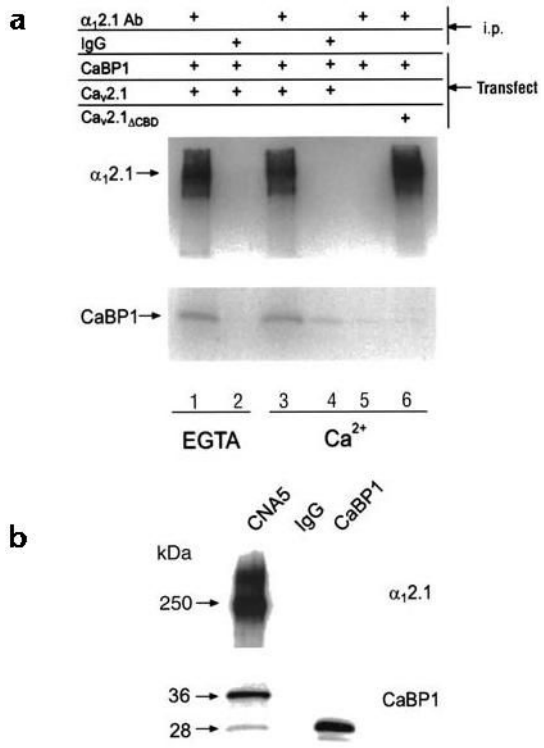

Fig. 2.

CaBP1 associates with the $\alpha_1$2.1 subunit in tsA-201 cells and rat brain. (**a**) Lysates from cells transfected with Ca_v2.1 plus CaBP, CaBP1 alone or $Ca_v2.1_{\Delta CBD}$ plus CaBP1 were subjected to immunoprecipitation (i.p.) with affinity-purified $\alpha_1$2.1-specific antibodies or control IgG as indicated. Experiments were done with 10 mM EGTA (lanes 1 and 2) or 2 mM Ca^{2+} (lanes 3–6). Blots were probed with $\alpha_1$2.1- (top) or CaBP1-specific antibodies (bottom). (**b**) Rat cerebellar proteins immunoprecipitated with $\alpha_1$2.1-specific antibodies (CNA5) or control IgG were immunoblotted with $\alpha_1$2.1- (top) or CaBP1-specific antibodies (bottom). Lysate from tsA-201 cells transfected with CaBP1 was used as a control.

NIH-PA Author Manuscript

NIH-PA Author Manuscript

NIH-PA Author Manuscript

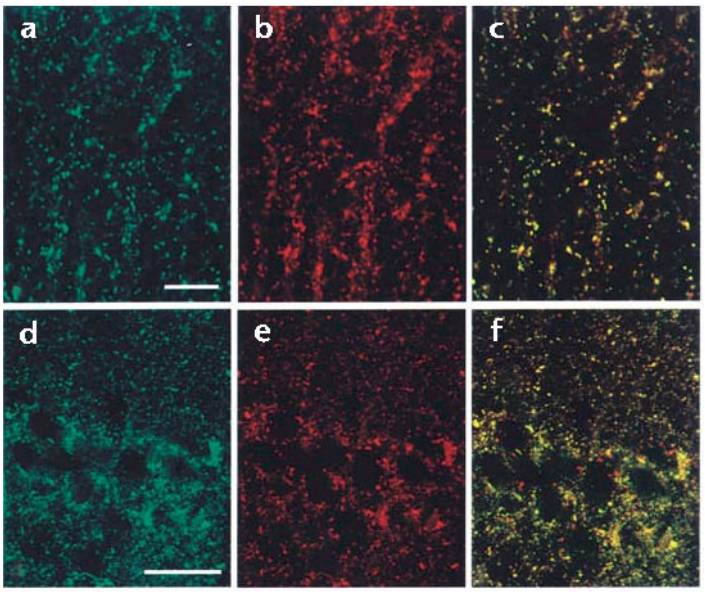

Fig. 3.

CaBP1 colocalizes with $\alpha_1$2.1 in rat brain sections. Rat brain sections were double-labeled with antibodies specific for CaBP1 and $\alpha_1$2.1. Labeling for CaBP1 is shown in green (**a**, **d**) and for $\alpha_1$2.1 in red (**b**, **e**). In the merged images (**c**, **f**), double-labeled structures appear yellow. Representative examples are shown from the molecular layer of the cerebellum (**a**–**c**) and the CA1 region of the hippocampus (**d**–**f**). Scale bars, 5 μm (**a**–**c**) and 50 μm (**d**–**f**).

NIH-PA Author Manuscript

NIH-PA Author Manuscript

NIH-PA Author Manuscript

Fig. 4.

CaBP1 enhances the inactivation of I_{Ca} in tsA-201 cells transfected with $Ca_v2.1$ channels. (**a**) Representative traces of I_{Ca} from cells transfected with $Ca_v2.1$ either alone (bottom) or with CaBP1 (top). Currents were evoked by 1-s pulses to the indicated voltages from a holding potential of −80 mV and were scaled for comparison. (**b**) Time constants for the inactivation of $Ca_v2.1$ channel currents in the absence of CaBP1. Test currents were evoked by pulses to the indicated voltages as described in (**a**) and fit with a single exponential function. Data were averaged from 6–18 cells. (**c**) Time constants for inactivation of I_{Ca} in cells cotransfected with CaBP1. Test currents were evoked by the same voltages as in (**a**) and (**b**), but current traces were fit with a double exponential function. Fast (τ_{fast}, filled bars) and slow time constants (τ_{slow}, open bars) were averaged from 7–20 cells.

NIH-PA Author Manuscript

NIH-PA Author Manuscript

NIH-PA Author Manuscript

Fig. 5.

Fast, Ca^{2+}-independent inactivation of $Ca_v2.1$ channels by CaBP1 differs from the modulation of $Ca_v2.1$ channels by CaM. (**a**) $Ca_v2.1$ channel currents recorded with Ca^{2+} or Ba^{2+} as the permeant ion. Test pulses were applied from a holding voltage of −80 mV to +10 mV (Ca^{2+}) or 0 mV (Ba^{2+}) for $Ca_v2.1$ either alone or cotransfected with CaM, or to +20 mV (Ca^{2+}) or +10 mV (Ba^{2+}) for cells cotransfected with CaBP1, to account for the positive shift in voltage-dependent activation caused by CaBP1. The intracellular solution contained 0.5 mM EGTA. (**b**) The residual current amplitude at the end of a test pulse (I_{res}, indicated in **a**) was normalized to the peak current (I_{pk}) for cells transfected with $Ca_v2.1$ either alone or with CaBP1 or CaM. (**c**) Representative currents evoked by a test pulse to +30 mV (+20 mV for I_{Ba}) in cells transfected with wild-type or mutant $Ca_v2.1$ lacking the CBD ($Ca_v2.1_{\Delta CBD}$) either alone or cotransfected with CaBP1. Intracellular solutions contained 0.5 mM EGTA except where 10 mM BAPTA is indicated and extracellular solutions contained 10 mM Ca^{2+} except where Ba^{2+} is indicated. (**d**) Current amplitudes at 200 ms (I_{200}, indicated in **c**) were normalized to the peak current (I_{pk}) and plotted for the different conditions. Recordings were from tsA-201 cells transfected with $Ca_v2.1$ or $Ca_v2.1_{\Delta CBD}$ either alone (open bars) or with CaBP1 (filled bars). Results represent averages of 5–13 cells. Asterisks indicate statistically significant differences between the paired groups ($p \leq 0.05$).

NIH-PA Author Manuscript

NIH-PA Author Manuscript

NIH-PA Author Manuscript

Fig. 6.

CaBP1 alters the voltage dependence of $Ca_v2.1$ activation. Tail current–voltage curves from tsA-201 cells transfected with $Ca_v2.1$ (**a**–**c**) or $Ca_v2.1_{\Delta CBD}$ (**d**) either alone (open circles) or with CaBP1 (filled circles). Test pulses (10 ms) to the indicated voltages were applied from a holding voltage of −80 mV and peak tail currents were measured upon the repolarization of cells to −40 mV, normalized to the largest tail current in the series, and plotted against test voltage. Test pulses were held for 10 ms, as activation of currents was complete but inactivation was minimal during this time. Bath solutions contained 10 mM Ca^{2+} (**a**, **c**, **d**) or Ba^{2+} (**b**), and intracellular solutions contained 0.5 mM EGTA (**a**, **b**, **d**) or 10 mM BAPTA (**c**). Each point represents the mean of 7–20 cells.

NIH-PA Author Manuscript

NIH-PA Author Manuscript

NIH-PA Author Manuscript

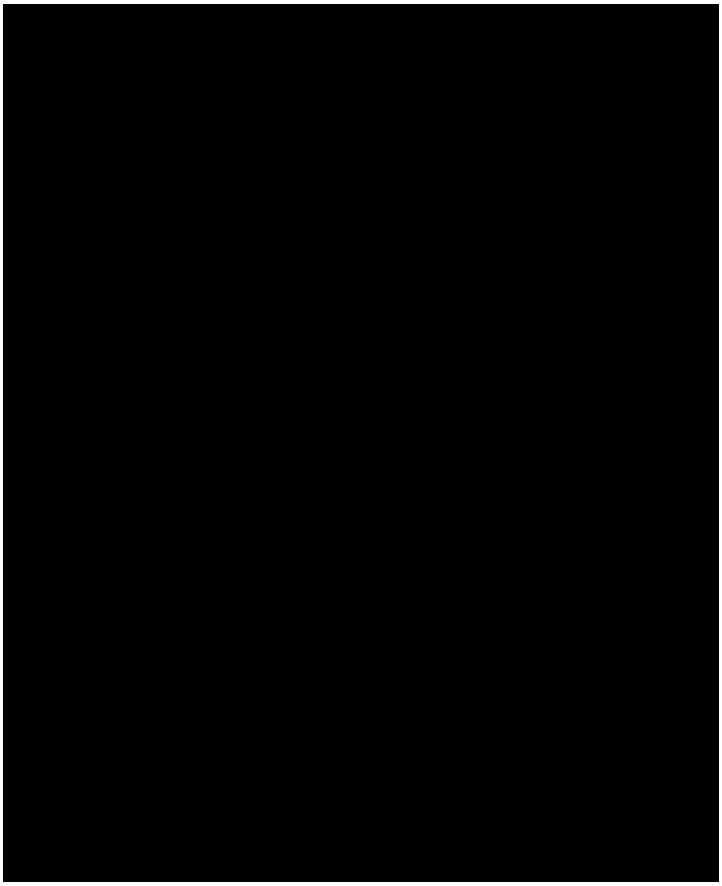

Fig. 7.

CaBP1 does not support Ca^{2+}-dependent facilitation of $Ca_V2.1$ channels. (**a**, **b**) Voltage dependence of $Ca_V2.1$ Ca^{2+} currents evoked before (P1, filled circles) and after (P2, open circles) a depolarizing prepulse. Tail currents were measured by repolarizing cells to −40 mV for 5 ms after variable test voltages and normalized to the largest tail current evoked by P1. Inset, representative currents evoked by a test pulse to +10 mV before (filled circles) and after (open circles) the prepulse. Intracellular recording solution contained 0.5 mM EGTA. Results were obtained from cells transfected with $Ca_V2.1$ either alone (**a**, $n = 7$) or with CaBP1 (**b**, $n = 10$). (**c**, **d**) $Ca_V2.1$ channel currents elicited by repetitive depolarizations. Test pulses (+20 mV (**c**) or +10 mV (**d**) to account for voltage shifts cause by Ba^{2+} substitution) at a frequency of 100 Hz were applied to cells transfected with $Ca_V2.1$ either alone (open circles) or along with CaBP1 (filled circles). Peak current amplitudes were normalized to the first pulse in the series and plotted against time during the train. Every second data point is shown. Intracellular recording solutions contained 0.5 mM EGTA, and bath solutions contained 10 mM Ca^{2+} (**c**) or Ba^{2+} (**d**). In (**c**), $n = 9$ for open circles; $n = 13$ for closed circles. In (**d**), $n = 5$ for open circles; $n = 11$ for closed circles.